JOURNAL OF APPLIED CRYSTALLOGRAPHY

ISSN 1600-5767

Multifitting: software for the reflectometric reconstruction of multilayer nanofilms

Mikhail Svechnikov*

Institute for Physics of Microstructures, Academicheskaya 7, Nizhny Novgorod, 603087, Russian Federation. *Correspondence e-mail: svechnikovmv@gmail.com

Received 18 October 2019
Accepted 23 November 2019

Edited by S. Boutet, SLAC National Accelerator Laboratory, Menlo Park, USA

Keywords: X-ray reflectometry; software; inverse problem; model structural reconstruction; multilayers.

Multifitting is a computer program designed specifically for modeling the optical properties (reflection, transmission, absorption) of multilayer films consisting of an arbitrary number of layers in a wide range of wavelengths. *Multifitting* allows a user to calculate the reflectometric curves for a given structure (direct problem) and to find the parameters of the films from the experimentally obtained curves (inverse problem), either manually or automatically. Key features of *Multifitting* are the ability to work simultaneously with an arbitrary number of experimental curves and an ergonomic graphical user interface that is designed for intensive daily use in the diagnosis of thin films. *Multifitting* is positioned by the author as the successor to the *IMD* program, which has become the standard tool in research and technology groups synthesizing and studying thin-film coatings.

1. Introduction

The characterization of a planar multilayer nanostructure is primarily a characterization of its one-dimensional geometry in terms of depth, *i.e.* the layer thickness and interface sharpness. The generally accepted and most widely used experimental technique for this is X-ray reflectometry (Russell, 1990). The speed and ease of measurement by laboratory diffractometers and the sensitivity of the method to differences in film thickness at the ångström level account for the popularity of this tool. A greater problem is the interpretation of the obtained data and the reconstruction of the dielectric profile of the sample. Over decades of use of the X-ray reflectometry technique, many methods have been developed to extract information about the structure of thin-film coatings from reflectometric data, both analytical and numerical (Hohage *et al.*, 2008; Zimmermann *et al.*, 2000). Currently, the main method of reflectometric analysis of curves is the construction of a model of the structure based on *a priori* information, general physical considerations, and the numerical adjustment of parameters such as the thickness, the density of layers, magnitudes of roughness and the thickness of interlayers on interfaces.

The numerical reconstruction of a multilayer structure involves a specialized computer program for calculating the reflection curves and controlling the parameters of the structure. In each group researching the reflection from multilayer coatings, it is likely that a similar program has been written, and often more than one. The reasons for this are varied: the lack of a publicly available tool or a lack of knowledge that

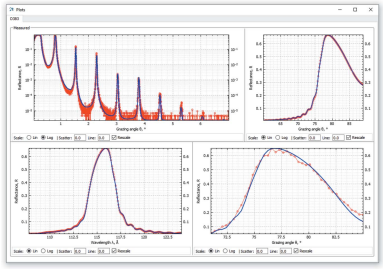

such a tool exists, the insufficient functionality of existing programs, an unwieldy user interface, a lack of documentation, the necessity of payment, or the preference of a researcher to program all the calculations by hand on principle. Sometimes, even if tasks are similar, the need to use additional data negates the possibility of using tools that have already been developed if they do not provide for such a possibility. These programs are then used by the team or by their authors and most often remain an internal product, inaccessible to other groups. Separately, it is worth mentioning that the program is often written by the author for a single task and is not supported or distributed in an ongoing way. It often does not have a friendly user interface or documentation, and working with the program involves working with its code. Thus, in order to repeat studies of structures such as those by Kozhevnikov *et al.* (2012), Zameshin *et al.* (2016) and Haase *et al.* (2016), the research team needs to follow a path of developing a suitable tool, even to implement an approach that is already known and approved.

In some cases, the program is published for a wide range of users. This could be a web service, for example those provided by the Center for X-ray Optics (CXRO), Lawrence Berkeley National Laboratory (http://henke.lbl.gov/optical_constants/), or Sergey Stepanov (https://x-server.gmca.aps.anl.gov), or a 'classic' program, for example *REFLEX* (Vignaud & Gibaud, 2019), *MOTOFIT* (Nelson, 2006), *GenX* (Björck & Andersson, 2007) or *IMD* (Windt, 1998). At the time of writing, *GenX* has been cited 396 times in scientific publications, and *IMD* 876 times. This means that such tools, with detailed documentation and a user-friendly graphical user interface, are still in high demand. It is particularly noteworthy that *IMD* has become the *de facto* standard reflectometric modeling tool in groups engaged in the development, synthesis and diagnostics of X-ray optical elements. Its key features are (i) the specification of a multilayer structure in the form of a tree with arbitrary nesting, (ii) the assignment of layer materials by substance name (if the corresponding dielectric constant is present in the database) or any combination of chemical elements with arbitrary stoichiometry and density, (iii) the description of the interlayer imperfections as corrections to the Fresnel coefficient reflection or by specifying the spectrum of roughness (power spectral density), (iv) the ability to automatically fit the reflection curve using both gradient and genetic algorithms, and (v) an extensive base of optical constants, consisting of atomic factors not only from CXRO but also collected from many other sources. However, like most other tools, *IMD* allows the user to work with only one experimental curve at a time, which particularly limits its use in characterizing reflective coatings at several wavelengths at once.

To a considerable degree, the *Multifitting* program was created for its ability to simulate a whole set of reflectometric curves simultaneously. Of course, this is not the only difference from *IMD*: high-speed calculations, a redesigned interface and new functionality are also included in the set. The main features of the *Multifitting* program and its layout from the user's point of view are presented in the following sections.

2. General organization of the program and main features

The design and main features of *Multifitting* were largely dictated by the work of the Department of Multilayer X-ray Optics at the Institute for Physics of Microstructures of the Russian Academy of Sciences, where it was created. This work includes the development, synthesis and diagnostics of multilayer mirrors and free-standing filters for the soft X-ray and extreme ultraviolet ranges. The main purpose of the program is to simulate the optical properties of the films, such as their reflection, transmission and absorption, depending on the angle of incidence and the wavelength of the probing radiation (the direct problem), and to find the parameters of the films on the basis of experimentally obtained reflection and transmission curves, both manually and automatically (the inverse problem). The specified planar structure may contain an ambient, a substrate, independent layers, periodic stacks with an arbitrary nesting depth, with a number of layers in a period greater than two, and aperiodic stacks. Each layer of this structure is characterized by a material, density, thickness and interface at the upper boundary of this layer. The material can be given by name (usually a chemical formula), if there are optical constants in the database, or may be composed of individual chemical elements with arbitrary stoichiometric ratios. *Multifitting* can use the *IMD* optical constants database, which was compiled from the atomic scattering factors of the first 92 chemical elements (Henke *et al.*, 1993) and independent studies of certain substances. When using the constants of tabulated substances, the relative density is used as a multiplier in front of the tabulated polarizability. When specifying an arbitrary composition of individual chemical elements, the absolute density of the substance is indicated in g cm^{-3}. The interlayer interface is characterized by the root mean square width, σ, and the type of profile described in the next section. The periodic structure can be characterized by the number of periods and the period thickness, and when the number of layers in the unit cell is two, the value of γ is also the ratio of the thickness of the first layer to the period thickness. For each layer in the unit cell, the deviation from the exact periodicity can be set, such as a linear, random or periodic addition to the thickness over the depth of the structure.

The number of experimental curves simultaneously taken into account for each structure is arbitrary. Each curve is characterized by the type of measured value (reflection/transmission/absorption), the type of argument (incidence angle/grazing angle/wavelength/photon energy), the units of measurement of the argument (degrees/minutes/second/radians/milliradians/ångströms/nanometres/micrometres/electronvolts/kiloelectronvolts), the intensity and polarization of the probe radiation, the energy, and the angular resolution of the device. For measurements at small grazing angles, the shape and width of the probe beam intensity profile, the sample size and its position relative to the beam are important. When calculating a model curve intended for comparison with experimental data, the calculation is performed for the same values of the argument and instrument settings.

Table 1
The base capabilities of *Multifitting* for the modeling of a layered structure.

This table presents only the base functionality and omits a multitude of minor features.

Layered structure can include	Substrate	Single layers	Periodic stacks	Aperiodic stacks	
Periodic stack can be characterized by	Number of periods	Period thickness	Thickness ratio	Thickness drift	Interface thickness drift
Layer can be characterized by	Material	Density	Thickness	Upper interface thickness	Upper interface shape
Each experimental curve can be characterized by	Argument type	Value type: R, T, A	Sample measurement geometry	Angular/spectral resolution of a probe beam	Polarization
Fitting algorithms	Gradient-based		Evolutionary	Other/mixed	
Number of curves	Arbitrary number of experimental data sets			Arbitrary number of modeled curves	

The number of structures calculated simultaneously can also be arbitrary. For a number of tasks where several structures have identical (or related) areas (for example, oxidized layers), their simultaneous reconstruction may be required under the condition of maintaining these relations. *Multifitting* allows the user to impose intra-structural and cross-structural relations between parameters.

A search of the model parameters can be performed manually or automatically. For automatic fitting, a range of possible values is specified for the variable structural parameters, *i.e.* the minimum and maximum values. The number of simultaneously adjusted parameters can be arbitrary. *Multifitting* contains several fitting algorithms implemented in the *GSL* (https://www.gnu.org/software/gsl) and *SwarmOps* (http://www.hvass-labs.org/projects/swarmops) libraries. It makes sense to divide these algorithms into two groups, that is, a local and a global search. Local search algorithms (primarily gradient algorithms) tend to converge to the local minimum of the residual near the initial point in the parametric space. However, their advantages are their rate of convergence and the accuracy of finding this local minimum. Global search algorithms (primarily evolutionary algorithms) require a large number of residual computations at numerous points in the parametric space and converge more slowly, but they check a much wider range of possible parameter values and have a higher probability of finding a sufficiently deep minimum of the residual. *Multifitting* allows the user to run a series of automatic fits with random initial values of the variable parameters. This strategy increases the coverage of the parametric space and increases the probability of success; however, it involves a proportional increase in the time for calculations.

To estimate the confidence intervals of values, the parameter is set to fixed values within a specified interval, and for each of these values, other variables are fitted. On the basis of the inverted bell-shaped (pit-like) distribution of the final values of the residual function, a conclusion is drawn about the allowable interval of the parameter values.

For ease of understanding and brevity, the base capabilities of *Multifitting* are given in Table 1.

Multifitting was developed in the C++ programming language for Windows and Linux, and all the necessary libraries are included in the distribution. *Multifitting* has been used in several prior studies (Chkhalo *et al.*, 2017; Svechnikov *et al.*, 2018, 2017; Nechay *et al.*, 2018; Barysheva *et al.*, 2019).

3. Computation methods

3.1. Plane waves in a layered structure

The calculation of the field of a plane wave in a one-dimensional piecewise-layered medium with sharp boundaries is an exactly solvable problem. This field can be recalculated from one boundary to another within the framework of recurrence relations (Parratt, 1954; Vinogradov *et al.*, 1989):

$$\begin{aligned} r(z_j) &= \frac{r_j^{\mathrm{F}} + r(z_{j+1})\exp(2i\chi_{j+1}l_{j+1})}{1 + r_j^{\mathrm{F}} r(z_{j+1})\exp(2i\chi_{j+1}l_{j+1})}, \quad j = 0 \ldots N, \\ r(z_{N+1}) &= 0, \\ t(z_j) &= \frac{t(z_{j+1})t_j^{\mathrm{F}}\exp(i\chi_{j+1}l_{j+1})}{1 + r_j^{\mathrm{F}} r(z_{j+1})\exp(2i\chi_{j+1}l_{j+1})}, \quad j = 0 \ldots N, \\ t(z_{N+1}) &= 1, \end{aligned} \tag{1}$$

where $r(z_j)$ and $t(z_j)$ are the complex reflection and transmission coefficients of a structure lying below the jth boundary, $\chi_j = k(\varepsilon_j - \cos^2\phi)^{1/2}$ is the z component of the wavenumber in the jth medium, ε_j is the permittivity of the jth layer, ϕ is the grazing angle of the probing radiation, and l_j is the thickness of the jth layer. $r(z_0)$ and $t(z_0)$ are the reflection and transmission of radiation for the structure as a whole. The z component of the wavenumber and the thickness of the layer appear in the exponent. r_j^{F} and t_j^{F} are the Fresnel coefficients of reflection and transmission of a wave through the material interface. A diagram of the reflection from the layered structure is given in Fig. 1.

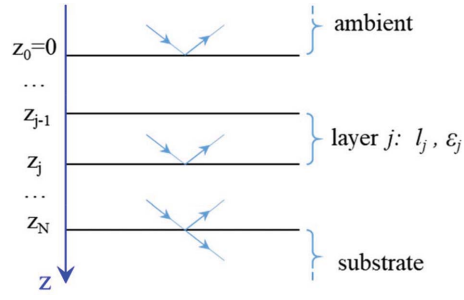

Figure 1
Reflection of a plane wave from a layered structure.

3.2. Interface imperfections: extended 1D model

The roughness at the interfaces and the effects of the interpenetration of materials due to diffusion, implantation and chemical interaction are taken into account with the help of a weakening factor at the Fresnel reflection coefficient. In accordance with Stearns (1989), if the dielectric constant profile at the interface changes from a value of ε_j to ε_{j+1} according to the law $p(z)$, then the reflection and transmission coefficients across the boundary are modified as follows:

$$\begin{aligned} r_j^{\rm F} &\rightarrow r_j^{\rm F}\tilde{w}\left[{\rm Re}(\chi_{j+1})\right], \\ t_j^{\rm F} &\rightarrow t_j^{\rm F}\tilde{w}\left[{\rm Re}(\chi_j-\chi_{j+1})\right], \end{aligned} \qquad (2)$$

where $\tilde{w}(q)$ is the Fourier transform of the profile derivative $w(q)={\rm d}p(z)/{\rm d}z$. The profile functions used and the corresponding Fourier factors are listed in Table 2. The profile plots are shown in Fig. 2.

Five profiles are available in *IMD*: 'erf', 'lin', 'exp', 'sin' and 'step'. However, only one profile can be selected for each interface. *Multifitting* allows a profile to be used that is a linear combination of all six profiles with individual weights α and widths σ:

$$f(z)=\frac{\sum \alpha_j f_j(z,\sigma_j)}{\sum \alpha_j}, \quad \alpha_j \geq 0, \quad \sum_j \alpha_j > 0, \qquad (3)$$
$$j = {\rm erf, lin, exp, tanh, sin, step}.$$

Thus, the shape of the profile is not fixed and can be controlled by parameters that are set manually or which can be found from the fitting results. This approach is physically motivated, since from general considerations it is clear that the transition layer model should reflect realistic situations. For example, if it is known that the main contribution to the transition region is caused by roughness, then the integral of the distribution function of the roughness heights should be used for determination of the transition layer shape. Recall that geometric roughness leads to a decrease in specular reflection, as if there is a smooth transition layer of the corresponding shape. However, a real transition layer is formed at the boundary of substances as a result of mechanical mixing during sputtering, chemical reactions and thermal diffusion. This transition layer may have its own form; for example, in Mo/Si mirrors, relatively homogeneous layers of Mo_xSi_y described by the 'step' function are formed at the boundaries (Yakshin *et al.*, 2000). The transition layer related to 'erf' corresponds to roughness with a Gaussian distribution of heights. A linear transition layer is formed by the simultaneous action of chemical interaction, diffusion and roughness, such as, for example, in multilayer mirrors based on La/B (Kuznetsov *et al.*, 2015; Andreev *et al.*, 2009; Makhotkin *et al.*, 2013).

Thus, the shape of the transition layer is determined by several independent physical processes simultaneously, and these shapes will differ for the same pair of materials with

Table 2
Profile functions and their corresponding Fourier factors.

Function name	Profile $p(z)$	Fourier $\tilde{w}(q)$
Error function ('erf')	$\frac{1}{2}\left[1+{\rm erf}\left(\frac{z}{2^{1/2}\sigma}\right)\right]$	$\exp(-2q^2\sigma^2)$
Linear ('lin')	$\begin{cases} 0, & z \leq -3^{1/2}\sigma \\ \frac{1}{2}+\frac{z}{2(3^{1/2})\sigma}, & -3^{1/2}\sigma < z < 3^{1/2}\sigma \\ 1, & z \geq 3^{1/2}\sigma \end{cases}$	$\frac{\sin[2(3^{1/2})q\sigma]}{2(3^{1/2})q\sigma}$
Exponential ('exp')	$\begin{cases} \frac{1}{2}\exp\left(\frac{2^{1/2}z}{\sigma}\right), & z \leq 0 \\ 1-\frac{1}{2}\exp\left(\frac{2^{1/2}z}{\sigma}\right), & z > 0 \end{cases}$	$\frac{1}{1+2q^2\sigma^2}$
Hyperbolic tangent ('tanh')	$\frac{1}{2}\left\{1+\tanh\left[\frac{\pi z}{2(3^{1/2})\sigma}\right]\right\}$	$\frac{2(3^{1/2})q\sigma}{\sinh[2(3^{1/2})q\sigma]}$
Sinusoidal ('sin')	$\begin{cases} 0, & z \leq -\gamma\sigma \\ \frac{1}{2}+\sin\left(\frac{\pi z}{2\gamma\sigma}\right), & -\gamma\sigma < z < \gamma\sigma \\ 1, & z \geq \gamma\sigma \end{cases}$ $\gamma=\pi/(\pi^2-8)^{1/2}$	$\frac{\pi}{4}\left[\frac{\sin(2\gamma q\sigma-\pi/2)}{2\gamma q\sigma-\pi/2}+\frac{\sin(2\gamma q\sigma+\pi/2)}{2\gamma q\sigma+\pi/2}\right]$ $\gamma=\pi/(\pi^2-8)^{1/2}$
Step function ('step')	$\begin{cases} 0, & z \leq -\sigma \\ \frac{1}{2}, & -\sigma < z < \sigma \\ 1, & z \geq \sigma \end{cases}$	$\cos(2q\sigma)$

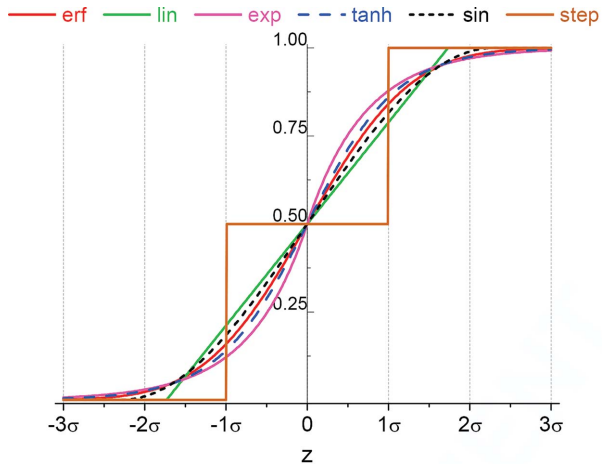

Figure 2
Plots of the profile functions shown in Table 2.

different layer thicknesses, at different temperatures and under different conditions of sputtering. In these circumstances, it is illogical to assume a single type of transition area, especially one that is coincident with some known 'simple' function. It seems more reasonable to use a linear combination of a predefined set of functions to determine the transition layer, in which the weights are fitting parameters. Each of the components can correspond to one or more of the physical processes that occur at the boundary during the formation, storage and operation of the multilayer coating. These components can be quite versatile (for example, the error function) or specific to particular materials (for example, a homogeneous step). It does not necessarily follow from the presence of a specific function in the selected set that it will contribute to the final profile; in the event that the assumed feature does not actually exist, the weighting coefficient of the corresponding function will turn out to have a small value in the reconstruction results. Our set should have the property of sufficiency, but not necessity. This fact allows us to approach the issue of choosing 'basic' functions less strictly, assuming only approximate distributions of the substance. The features of such an interface model are described in more detail in the paper by Svechnikov *et al.* (2017).

Representation of total profile as the sum of Fourier transforms of each function is allowed in the case of low reflectivity. Thus, it works almost everywhere for hard X-rays outside the area of total external reflection. But the main limitation for the use of damping reflection factors is 'non-overlap' of the lower and upper interfaces of each layer. According to Fig. 2, this means that the thickness of layers l_i should be $l_j > 2(\sigma_{\text{bottom boundary}} + \sigma_{\text{top boundary}})$, where $\sigma_{\text{bottom boundary}}$ and $\sigma_{\text{top boundary}}$ are the roughness/diffuseness r.m.s. at the top and bottom boundaries of the jth layer. This condition is common for using the sum of profile functions or a single function on the corresponding interface, and it limits the thickness of layers from below. Violation of this condition may lead to unreliable calculation for thin-layer systems with thick interfaces. Currently *Multifitting* uses only damping factors to consider interface imperfections, but in future it will perform an 'honest' fragmentation of dielectric constant profile and the aforementioned restriction will disappear.

3.3. Fitting algorithms

Finding the parameters of the model structure to match the simulated and measured (or target) reflectivity/transmissivity curve is one of the most important tasks that needs to be solved using programs similar to the one described in this paper. A preliminary (and also final) selection of the model and its approximate parameters based on *a priori* information and a visual assessment of the curves is always done manually, but if the number of essential parameters of the model is large enough (say more than three), then a manual search for a suitable parameter area in the parametric space within which the desired values may lie becomes too complicated and can take an unreasonable amount of time. The search for such 'target areas' is best done automatically. To achieve this, a metric is introduced in the space of reflectometric curves (this is also known as the mismatch function, discrepancy, goodness of fit, residual function, merit function or fitness function) that determines the distance, *i.e.* the numerical difference, between the curves. The residual functional determines the quantitative difference between the target and the calculated curves for given values of the parameters. The problem of coincidence of curves is actually replaced by the problem of minimizing the residual. However, these tasks are not always equivalent: for an incorrectly chosen residual, its minimum may correspond to a significant visual mismatch of the curves. The appropriate residual depends on the quality of the measurements, on the degree of adequacy of the model used in the calculation, and on the understanding of the problem by the researcher with regard to which differences between the curves can be neglected and which cannot. *Multifitting* provides considerable freedom in this regard. The residual can be specified in a standard χ^2 form, which is suitable for a normal distribution of measured signal values around the 'true' values, a small dynamic range of data, and good agreement between the model and experimental data:

$$\chi^2 = \frac{1}{n-m}\sum_{\text{curves}} w_{\text{curve}} \left\{ \sum_{\text{points}} \frac{\left[R^{\text{calc}}_{\text{curve}}(\lambda,\theta,\mathbf{p}) - R^{\text{exp}}_{\text{curve}}(\lambda,\theta)\right]^2}{\sigma^2} \right\}, \tag{4}$$

where the summation is carried out over all curves and within each curve over all its points, $\mathbf{p}$ represents the model parameters, λ the wavelength, θ the grazing angle, R_{curve} the experimental or calculated reflection coefficient, and σ the experimental uncertainty at a given point. With Poisson noise at the detector, we can assume that $\sigma^2 = R^{\text{calc}}_{\text{curve}}(\lambda,\theta,\mathbf{p})/I_0$, where I_0 is the probe beam intensity. w_{curve} is the weight of the curve, which is initially equal to one, and which allows a balance to be maintained if necessary between the contributions of different curves to the value of the residual. If χ^2 is not suitable, a residual in a fairly general form can be specified:

$$\text{residual} = \sum_{\text{curves}} \left\{ \sum_{\text{points}} \left| f_{\text{curve}}\left[R^{\text{calc}}_{\text{curve}}(\lambda,\theta,\mathbf{p})\right] - f_{\text{curve}}\left[R^{\text{exp}}_{\text{curve}}(\lambda,\theta)\right] \right|^n \right\}, \tag{5}$$

where n is a natural number and f_{curve} is a function that determines the type of residual for each curve and can be specified as an arbitrary combination of elementary functions.

The Levenberg–Marquardt algorithm from the *GSL* library and the differential evolution algorithm from the *SwarmOps* library are used to minimize the residual in *Multifitting*. The Levenberg–Marquardt algorithm quickly finds the 'nearest' local minimum in a parametric space, while the differential evolution algorithm covers a much larger area of parameters but converges more slowly. For larger coverage of the parametric space, a multiple-start algorithmic process from random starting points is implemented. In addition to finding a sufficiently deep minimum, this allows us to find several possible values of the parameters corresponding to the task,

the choice between which is done manually, on the basis of criteria other than the specific value of the residual.

4. User interface

When first using unfamiliar software, the 'intuitiveness' of the interface plays a major role, that is, the ability of the user to independently guess and remember how to carry out each operation. The documentation also plays a crucial role here. For an experienced user, other factors become important, such as the ease of access to the main parameters, the ease of making changes and the number of actions required for this. In this case, the more intensive the work with the program, the greater the user's need for a well-designed interface. If the program is intended for daily intensive use, special attention should be paid to its ergonomics. This section describes the graphical user interface and the reasons for its design.

4.1. Main window

The number of parameters involved in the structures, experimental and model curves, and graphs is huge, and it would not be feasible to present these to the user at the same time. *Multifitting* therefore has a multi-window interface, much like the *IMD* interface. This allows users to keep only the necessary windows open, and to arrange them conveniently in the case of a two-monitor configuration.

Basic structure management and access to other tools and options are available from the main program window (Fig. 3). The main window contains the studied structure in the form of a tree, which gives a general view of the structure and provides basic information about the parameters of the layers. Below this is a toolbar that allows the user to add or remove structure elements, and gives lower-level access to graph visualization, calculation and fitting settings ('Main Tools') and windows for defining 'independent' curves that are not related to experimental data ('Independent Variables'). At the very bottom ('Target Curve') there is a list of loaded experimental curves with a brief description and buttons for editing.

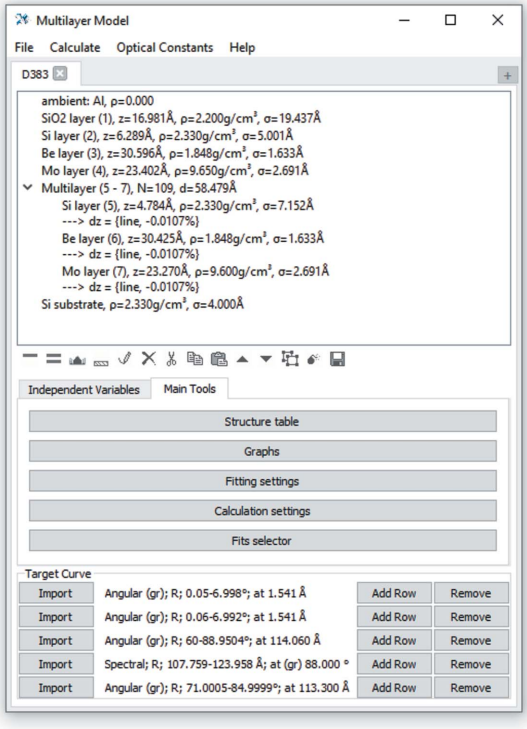

Figure 3
The main window of *Multifitting*. As an example, the structure of Mo/Be/Si is loaded.

4.2. Structure Item window

Double-clicking on the structure element opens a window that allows editing of the parameters of a stack, layer or substrate. The appearance of the windows is shown in Fig. 4. The SiO_2 layer (used here as an example) is composed of individual chemical elements, and the absolute density is given. For each layer, the thickness, the root mean square thickness of the transition layer ('Roughness/Diffuseness') and its shape ('Interlayer Composition') are also specified. The parameters of the periodic structure are the period thickness and the number of repetitions. There is also the possibility of inverting the order of the layers in the stack and turning the periodic structure into an aperiodic one.

Aperiodic stacks in *Multifitting* may be one of two types: 'General Aperiodic' and 'Regular Aperiodic'. The layers contained in the 'General Aperiodic' menu can be set completely independently, like layers outside of any stacks. The 'General Aperiodic' toolbar allows the user to quickly invert the sequence of layers if necessary, to quickly create or remove links between the parameters of layers consisting of the same materials, and to enable/disable the fitting of layer parameters on a large scale. The 'Regular Aperiodic' type allows the user to consider layers not as completely independent, but as differing from a strictly periodic structure only

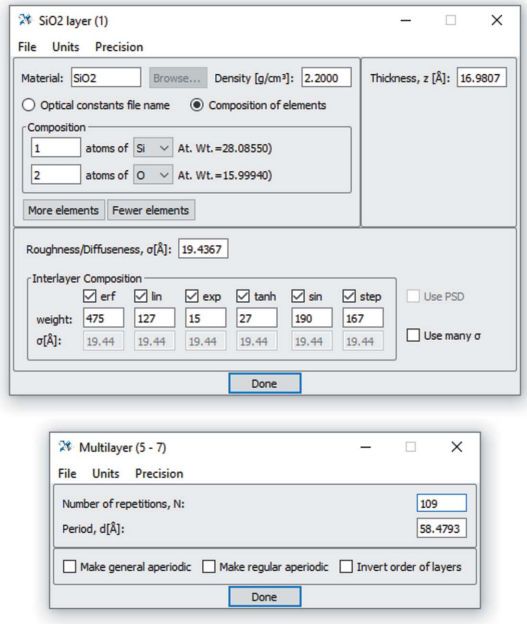

Figure 4
Windows for editing a separate layer and periodic structure.

in terms of their thicknesses and (if necessary) interfaces. In this case, it is possible to impose restrictions on the thickness variation during the automatic optimization of the mirror for the target reflection curve. The limitation on thickness variation may be required for technological reasons, such as if it is impossible to accurately calibrate the deposition machine for a wide range of layer thicknesses. In this case, the problem for which an aperiodic mirror is created can often be effectively solved over a limited range of thicknesses. The General Aperiodic and Regular Aperiodic windows are shown in Fig. 5.

4.3. 'Regular Aperiodic' window

A separate window allows for convenient work with individual layers inside the Regular Aperiodic menu (Fig. 6). The values of the layer thicknesses and interface thicknesses can be changed collectively for the layers in all unit cells as well as individually. The user can also select the layers involved in optimization or reconstruction. The presence of all layers in one compact table makes it possible to identify the dependence of the reflective properties of the structure on each thickness and interface of the individual layers, and in particular to observe the sensitivity of the reflection curve to layers at different depths of the multilayer structure.

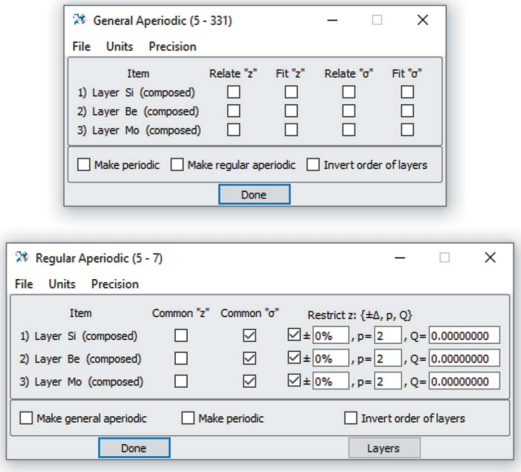

Figure 5
The 'General Aperiodic' and 'Regular Aperiodic' windows.

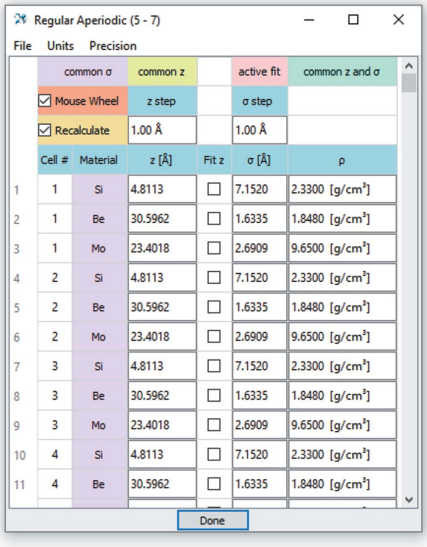

Figure 6
Window for 'Regular Aperiodic' layers.

4.4. 'Calculation Settings' window

The parameters for calculating and displaying all the curves, both loaded experimental/target and 'independent', are set in a special window. Any curve can be included/excluded from consideration. For each curve, the type of residual and the weight coefficient of the given curve are indicated, giving a corresponding contribution to the total residual. The function itself is set in text form in accordance with the valid syntax. A screenshot of the window is shown in Fig. 7.

4.5. 'Plots' window

The graphs of the curves marked in the 'Calculation Settings' window are displayed in a common window, which allows the user to see the entire set simultaneously. The observed discrepancy between the model and the individual experimental curves makes it possible to balance the contribution of each curve to the total residual and to find a compromise model that can satisfactorily describe the entire family of curves at once. Each curve can be displayed on a linear or logarithmic scale with fast switching between them. When the structure is changed and recalculated, the curves in the graphs are automatically updated. The ability to turn autoscaling on and off when recalculating also allows the user to follow the individual small sections of the curves in detail. The mutual positions of the curves relative to each other are also adjustable. An example of these graphs is shown in Fig. 8.

4.6. 'Table Of Structures' window

The multilayer structure involves a huge number of parameters that need to be set and changed during the modeling

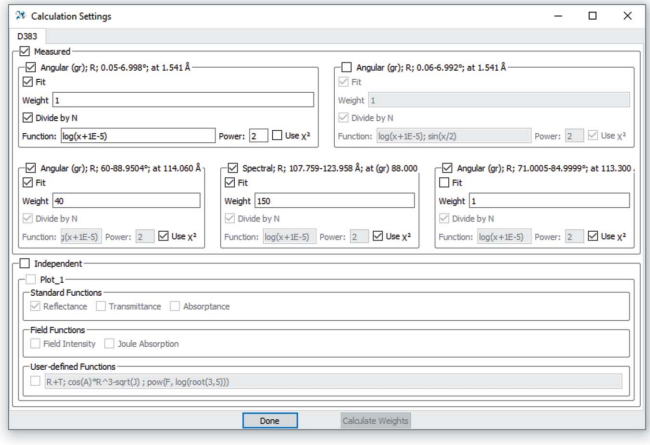

Figure 7
Window of parameters for displaying all curves and setting individual residuals.

process. Each layer is characterized by more than ten values, including the density, stoichiometry, thickness, width and shape of the interface, and the magnitude and type of drift in the composition of the quasi-periodic stack. In addition to this, each variable parameter has upper and lower boundaries and an 'on/off' checkbox. Thus, structures with even a small number of layers (not counting the substrate) already have more than a hundred adjustable parameters, and the operative access to these determines the convenience and functionality of the modeling tool. To solve this problem, a special table was created in *Multifitting* that displays this entire array of parameters in a structured way. In terms of its organizational and informational load, this table is the most complex element of the interface, but at the same time it is one of the most valuable in terms of functionality. A screenshot of this table is shown in Fig. 9.

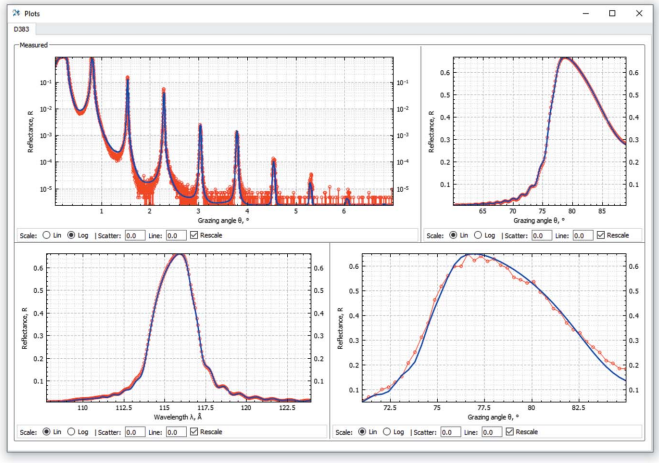

Figure 8
Graphs of experimental and calculated curves.

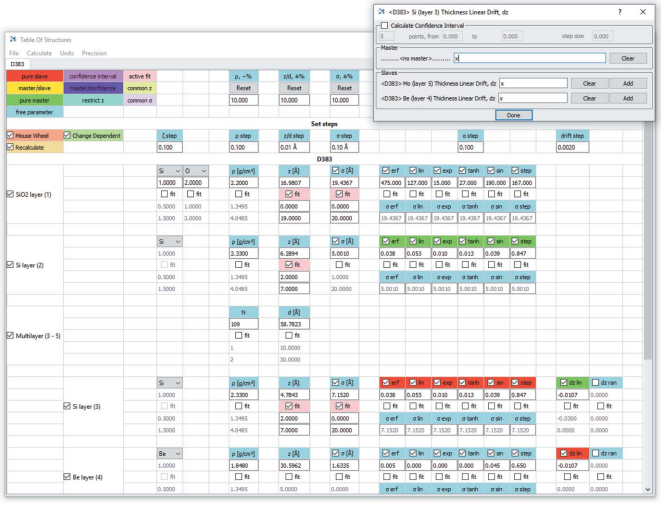

Figure 9
A detailed table that allows the user to work with the structure, changing its parameters, setting intervals of allowable values for fitting and imposing relations between parameters. A window for managing the relations of a particular parameter is shown in the upper right.

In addition to controlling the parameters listed above, the table allows the user to temporarily turn off individual layers and whole stacks from consideration, to set valid intervals on a large scale for the values of variable parameters as percentages of the current values, and to impose connections between parameters. The convenience of imposing relations (and, importantly, their tracking) is associated with another degree of freedom of the graphical interface, which is actively involved here: color. The use of colored cells allows users to quickly find variables and related parameters. In the upper left-hand corner of the table is a legend that briefly describes the role of a particular color.

A separate system for managing relations of parameters to each other is implemented within the framework of this general table. A 'coupling' window can be opened for each parameter in the table, allowing the user to specify its dependencies and to search for a confidence interval (upper right-hand corner of Fig. 9). The type of dependence can be arbitrary, involving any combination of elementary functions. The physical meaning of this relationship and the possibility of nonphysical values (for example, negative ones) are not checked and their correctness remains at the discretion of the user. For each parameter, there are two types of links, the 'master' and 'slave'. The 'slave' value is calculated from the 'master' value: slave = f(master). Accordingly, each parameter can have at most one 'master' on which it depends, but any number of 'slaves' that depend on it. Thus, whole chains of dependencies can be constructed, and these are calculated at each iteration of the fit or when the parameters are changed manually. In accordance with the status of each parameter participating in the chain, it is colored green, yellow or red.

4.7. 'Fits Selector' window

A very convenient feature of *Multifitting* allows the user to save the current configuration of the structure, *i.e.* the layers and all their parameters and dependencies, so that the user can

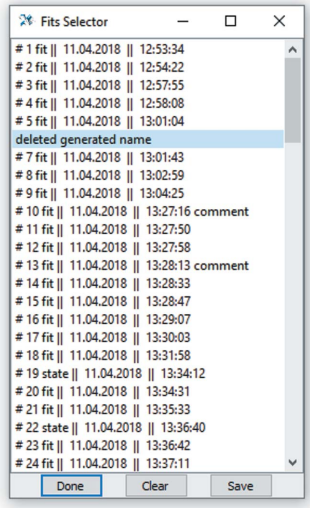

Figure 10
Window of the saved states of the structure, allowing quick access to good configurations.

quickly return to it at any moment. The state of the structure before and after the automatic fit is also saved, as are the results of all fittings with repeated starts from random starting points. This allows the user to quickly assess the effectiveness of the automatic fit and, in some cases, when the result is poorer, to return to the starting position. As can be seen in the screenshot of the 'Fits Selector' window (Fig. 10), each state is assigned an automatically generated name containing the type of saving (manual or automatic at the fitting), the date and the time of creation. The names are editable, allowing the user to mark specific configurations.

5. Summary and future developments

This paper describes the main features of the *Multifitting* program and the features of its interface that are most important to the end user. The program is likely to be of particular interest to researchers engaged in the development, creation and diagnostics of X-ray optical coatings and free-standing foils, as well as to those engaged in the synthesis and diagnostics of quantum walls for nanoelectronics. The long-term experience of the team has been invested in the development of this software, which is designed to solve the inverse problem of reflectometry. For this reason, the program has a number of features that are not evident at first use, but which have a great impact on its simplicity and ease of use. Because special attention has been paid to the ergonomics of the program in various use scenarios, we urge current and potential users to send requests regarding both its functionality and its user interface so that these requests can be taken into account. *Multifitting* is being actively developed, old errors are being corrected and new possibilities are being added, and we hope that this program will find wide application as a tool for the X-ray diagnostics of multilayer coatings.

6. Distribution

Multifitting is freeware and can be downloaded from http://xray-optics.org/products/software-multifitting/. It can be run under Windows and Linux; all necessary libraries are included in the distribution.

Funding information

This work was carried out in the framework of state project No. 0035-2014-0204, with support from the Russian Foundation for Basic Research (RFBR) (18-32-00173).

References

Andreev, S. S., Barysheva, M. M., Chkhalo, N. I., Gusev, S. A., Pestov, A. E., Polkovnikov, V. N., Salashchenko, N. N., Shmaenok, L. A., Vainer, Y. A. & Zuev, S. Y. (2009). *Nucl. Instrum. Methods Phys. Res. A*, **603**, 80–82.

Barysheva, M. M., Garakhin, S. A., Zuev, S. Y., Polkovnikov, V. N., Salashchenko, N. N., Svechnikov, M. V., Chkhalo, N. I. & Yulin, S. (2019). *Quantum Electron.* **49**, 380–385.

Björck, M. & Andersson, G. (2007). *J. Appl. Cryst.* **40**, 1174–1178.

Chkhalo, N. I., Gusev, S. A., Nechay, A. N., Pariev, D. E., Polkovnikov, V. N., Salashchenko, N. N., Schäfers, F., Sertsu, M. G., Sokolov, A., Svechnikov, M. V. & Tatarsky, D. A. (2017). *Opt. Lett.* **42**, 5070–5073.

Haase, A., Bajt, S., Hönicke, P., Soltwisch, V. & Scholze, F. (2016). *J. Appl. Cryst.* **49**, 2161–2171.

Henke, B. L., Gullikson, E. M. & Davis, J. C. (1993). *At. Data Nucl. Data Tables*, **54**, 181–342.

Hohage, T., Giewekemeyer, K. & Salditt, T. (2008). *Phys. Rev. E Stat. Nonlinear Soft Matter Phys.* **77**, 1–9.

Kozhevnikov, I. V., Peverini, L. & Ziegler, E. (2012). *Phys. Rev. B*, **85**, 125439.

Kuznetsov, D. S., Yakshin, A. E., Sturm, J. M., van de Kruijs, R. W. E., Louis, E. & Bijkerk, F. (2015). *Opt. Lett.* **40**, 3778.

Makhotkin, I. A., Zoethout, E., van de Kruijs, R., Yakunin, S. N., Louis, E., Yakunin, A. M., Banine, V., Müllender, S. & Bijkerk, F. (2013). *Opt. Express*, **21**, 29894–29904.

Nechay, A. N., Chkhalo, N. I., Drozdov, M. N., Garakhin, S. A., Pariev, D. E., Polkovnikov, V. N., Salashchenko, N. N., Svechnikov, M. V., Vainer, Y. A., Meltchakov, E. & Delmotte, F. (2018). *AIP Adv.* **8**, 075202.

Nelson, A. (2006). *J. Appl. Cryst.* **39**, 273–276.

Parratt, L. G. (1954). *Phys. Rev.* **95**, 359–369.

Russell, T. P. (1990). *Mater. Sci. Rep.* **5**, 171–271.

Stearns, D. G. (1989). *J. Appl. Phys.* **65**, 491–506.

Svechnikov, M. V., Chkhalo, N. I., Gusev, S. A., Nechay, A. N., Pariev, D. E., Pestov, A. E., Polkovnikov, V. N., Tatarskiy, D. A., Salashchenko, N. N., Schäfers, F., Sertsu, M. G., Sokolov, A., Vainer, Y. A. & Zorina, M. V. (2018). *Opt. Express*, **26**, 33718–33731.

Svechnikov, M., Pariev, D., Nechay, A., Salashchenko, N., Chkhalo, N., Vainer, Y. & Gaman, D. (2017). *J. Appl. Cryst.* **50**, 1428–1440.

Vignaud, G. & Gibaud, A. (2019). *J. Appl. Cryst.* **52**, 201–213.

Vinogradov, A. V., Brytov, I. A., Grudsky, A. Y., Kogan, M. T., Kozhevnikov, I. V. & Slemzin, V. A. (1989). *Zerkal'naya Rentgenovskaya Optika (X-ray Mirror Optics)*. Leningrad: Mashinostroenie.

Windt, D. (1998). *Comput. Phys.* **12**, 360.

Yakshin, A., Louis, E., Görts, P., Maas, E. L. & Bijkerk, F. (2000). *Physica B*, **283**, 143–148.

Zameshin, A., Makhotkin, I. A., Yakunin, S. N., van de Kruijs, R. W. E., Yakshin, A. E. & Bijkerk, F. (2016). *J. Appl. Cryst.* **49**, 1300–1307.

Zimmermann, K.-M., Tolan, M., Weber, R., Stettner, J., Doerr, A. K. & Press, W. (2000). *Phys. Rev. B*, **62**, 10377–10382.